A PROPOSED METHOD FOR THE INVERSE PROBLEM IN ELECTROCARDIOLOGY

M. S. LYNN, A. C. L. BARNARD, J. H. HOLT,
and L. T. SHEFFIELD

From the IBM Scientific Center, Houston, Texas 77025 and the Department of Medicine, Medical College of Alabama, Birmingham, Alabama 35233

ABSTRACT The inverse problem in electrocardiography is considered. A method is proposed in which the cardiac electrical generator is represented by a set of dipoles, fixed in location and direction in order to reflect the known features of myocardial excitation, but variable in strength. A crucial innovation is that since the dipole directions have been so chosen, the dipole strengths must be constrained nonnegative. Surface potentials are measured in vivo and the dipole strengths inferred. In this process, torso models with a varying degree of realism are used. An 11-dipole set is used and potentials are measured at 126 surface locations. For a particular normal subject, the effect of various variables, such as the torso modeling assumptions, on the dipole strengths is investigated. Condensed results are given for twelve normal subjects and two patients.

INTRODUCTION

In (1, 2) we discussed the "forward" problem of electrocardiography, i.e., to determine the potential distribution over the surface of the thorax produced by a given cardiac electrical source. Models of the torso were employed which took into consideration the external torso boundary and major internal electrical inhomogeneities (the cardiac blood masses and the lungs). The given sources consisted of dipoles located in the myocardium. In the present paper we consider the "inverse" problem of electrocardiography, i.e., given surface potentials recorded in vivo at a finite number of locations on the thoracic surface, "characterize" the generating source in order to deduce the myocardial condition.

There are an infinite number of possible schemes for such characterizations, including, of course, the models of conventional electrocardiography. Although some extensions have been proposed, the body is usually considered as (see reference 18 for a complete bibliography) an electrically unbounded or (in defining corrected orthogonal lead systems) bounded homogeneous medium and the source

as a single equivalent generator, usually a dipole [but see (6, 10, 17) for example], fixed in location but not in orientation. These simplified models are attractive, not only because they have become well-established in practice, with a vast associated backlog of experience, but also because their implementation requires potential recordings at only a small number of sites and readily available inexpensive equipment.

Recently (5, 11, 13, 14, 22, 26, 27) there has been interest in recording potentials at a large number of surface sites, using analog-to-digital techniques and digital computers to process and analyze these large amounts of data. Hopefully the additional information and flexibility would lead to characterizations from which improved diagnoses could be made. The improvement might be in accuracy, in detail, or in ease of interpretation. Whether or not such improvements can in fact be obtained is unknown at present, and in this paper we make no claims whatsoever about the practical usefulness of our work. Rather, we shall present a particular method, together with some evidence to suggest that this or some similar method merits further investigation.

There are obviously many directions in which one might proceed. In order to simulate the "forward" problem, Selvester, Collier, and Pearson (25) proposed dividing the ventricular myocardium into twenty segments. Each segment is then represented, for electrical purposes, by a single dipole whose direction is fixed to be the expected average direction of propagation of the depolarization wave in that segment. Thus the dipoles point generally outward in the free walls, in accordance with the depolarization sequence established by work with penetrating electrodes (see references 20 and 21 for example). As time progresses and the depolarization wave front moves through a particular segment, the strength of the dipole representing that segment would be expected to rise to a maximum and then fall off. It follows directly from the considerations of (25) that it would be expected that the area under the strength-time curve for a particular dipole would be proportional to the volume of viable myocardium in that segment, assuming a constant rate of propagation of the depolarization wave. A highly constrained approach to the inverse problem was suggested in reference (4), a simulation which also suffers from a lack of uniqueness. A further simulation using unconstrained least-squares fitting (see Method) was reported in reference 13.

There is a unique solution to the latter formulation of the inverse problem, that is, given a set of source dipoles and sufficient surface potential data, determine the dipole strengths that give a best fit in the least-squares sense to these data. We have, however, not found this approach to be satisfactory when applied to in vivo data (see Dipole Strength Results). A radical modification to this technique (discussed in this paper) is necessary. This leads to a somewhat different interpretation of the multiple-dipole approach (see Method).

Horan and Flowers (11) have proposed a model employing a 233 dipole set. The QRS period is divided into seven intervals and each dipole is constrained to

be either "on" or "off" with a fixed strength during each interval. The permissible on-off sequence of each dipole is constrained to single square-wave configurations. A solution to the inverse problem is obtained by employing an iterative search technique to determine those dipole sequences which result in a particular best approximation to the surface data. However, this constrained approach is considerably underdetermined. Thus, the solutions are not unique, and depend upon the starting point. Nevertheless, interesting results with in vivo canine data were obtained with this model.

Our over-all purpose in this paper is to describe our method and present some results to show why we consider that it merits further study. Some preliminary clinical results were announced (14).

METHOD

We first consider the mathematical statement of our method for the inverse problem. Let the potential "transferred" to the ith surface location by a unit-strength dipole at myocardial location k be T_{ik}. Here $i = 1, \cdots, I$ and $k = 1, \cdots, K$, where I = total number of surface locations and K = total number of dipoles. If we have a set of dipoles with known strengths, d_k, then using the superposition principle the potential transferred to the ith surface location is $\sum_k T_{ik} d_k$. This is the "forward problem". In the present formulation of the "inverse problem," we are given the potentials v_i at the surface location i and we wish to determine the strengths d_k such that

$$\sum_{i=1}^{I} \left(v_i - \sum_{k=1}^{K} T_{ik} d_k \right)^2$$

is a minimum (if the model were precise and the data "noise-free," this minimum would be zero). In matrix notation, we minimize the Euclidean length of

$$(\mathbf{v} - \mathbf{Td})$$

where $\mathbf{T}$, the elements of which were defined above, is the "transfer matrix" with I rows and K columns, and $\mathbf{v}$ and $\mathbf{d}$ are column matrices. $\mathbf{T}$ is precomputed and depends upon the assumptions concerning electrical inhomogeneities (see Models for the Torso); we have considered this somewhat complex computational problem in (2, 15, 16) (see also references 3, 7–9).

This minimization problem has a unique solution if I is at least as large as K (assuming that $\mathbf{T}$ has rank K). In practice, to overcome problems of numerical instability, noise in the data, and model limitations, I has to be considerably larger than K. That is, we must considerably overdetermine the problem.

Since the surface potentials and dipole strengths are time-varying, such a minimization problem is posed at each of the J time intervals over which the surface potential is sampled. Mathematically, this is equivalent to minimizing

$$\sum_{j=1}^{J} \sum_{i=1}^{I} \left(v_{ij} - \sum_{k=1}^{K} T_{ik} d_{kj} \right)^2$$

where, now v_{ij} is the measured potential at the ith location over the jth time interval and d_{kj} is the kth dipole-strength during that time interval.

The solution for each time interval is both unique and independent of the solution for any other time interval, that is, we impose no time constraints on our solution. Thus, we infer the depolarization sequence as a result of our analysis and not as a consequence of imposed time constraints. (We note that time-constraints are inherent in the approaches given in references 4 and 11). We shall call this the *unconstrained* approach since the dipoles, while fixed in location and orientation, are not constrained in either time or strength. However, we have found the completely unconstrained approach to give unreliable results (see Dipole Strength Results). We therefore impose one constraint to reflect the normal depolarization sequence from endo- to epicardium, that is, we constrain the dipole strength to be nonnegative,

$$d_{kj} \geqq 0 \ (k = 1, \cdots K; j = 1, \cdots J).$$

With this constraint, our minimization problem mathematically changes from one of least-squares fitting (or multiple regression) to one of quadratic programming, and may be solved by the method of Wolfe (28). We note that the solution to this problem is still unique. This constraint, which appears not to have previously been considered in the literature, is, we feel, crucial to the multiple-dipole approach.

In the conventional interpretation of the scalar ECG or of the vectorcardiogram (VCG), the single equivalent generator represents the vector sum of the electrical sources (18). Thus, for example, it is often difficult to distinguish between a posterior infarction in the left ventricle and high activity in the right ventricle. The failure we experienced with unconstrained fitting is also due to inability to separate spatial components.

In our approach we attempt to factor the source into its constituent spatial and directional components, using the constraint of nonnegativity together with spatial separation of the dipoles. The objective is to associate each component with a particular area of myocardium, at least in normal subjects. This factoring of the electrical source into its separate components raises new fundamental possibilities in electrocardiographic diagnosis, including that of separating right from left ventricular activity. This is discussed more fully under Discussion of the Activation Sequence.

The work reported in this paper is confined to ventricular depolarization. With the present state of development of our procedures, we have found it convenient to work with a set of eleven dipoles with continuously-varying strengths. All results in this paper are based on this set. The dipoles are oriented consistent with the philosophy of (25), that is in the expected average direction of propagation of the depolarization wave in the represented segment. The exception to this is the omission of the right-pointing activity in the septum, which we have thus far found hard to separate from the activity in the right ventricle free wall (see Discussion of the Activation Sequence). Three dipoles are located in the septum, one at the apex, four in the left ventricle free wall, and three in the right ventricle free wall. The locations, direction, and names of the eleven dipoles appear in Table I, and the myocardial segments they represent are indicated in Fig. 1. We recognize that this set may not be optimal and may be changed in future work. It is probable, for example, that the high activity displayed on dipole 1 (in the posterior basal septum) should be further factored into at least two separated dipoles. We might remark that we believe that it is not so much the number of dipoles that is important (a 20-dipole set was considered in reference 25, a 233 dipole set in reference 11), but the methodology employed in inferring their strengths from the surface potentials.

At the time of writing, surface potentials have been measured on twenty normal subjects and sixteen patients. Since clinical papers will appear elsewhere, in the present paper we shall mention only briefly the variations from subject to subject, and the effect of various pathologies on the dipole strength curves. We shall concentrate on measurements on a single subject and show how variables such as the torso modeling assumptions and lead placement

TABLE I

11 DIPOLE SET

x, y, and z give the coordinates in meters of the dipole location. The x axis points frontward, the y axis to the left, and the z axis upward. The origin is at the umbilicus. l, m, and n are the corresponding direction cosines.

Number	Name	x	y	z	l	m	n
1	Posterior basal septum	0.045	0.005	0.222	−0.904	−0.301	−0.301
2	Apex	0.095	0.060	0.222	0.707	0.707	0.0
3	Anterior basal septum	0.075	0.035	0.253	0.805	0.563	0.187
4	Apical septum	0.085	0.035	0.212	0.929	0.310	−0.200
5	Lower anterior lateral LV	0.070	0.065	0.218	−0.097	0.621	−0.777
6	Anterior mid LV	0.067	0.060	0.243	0.119	0.954	0.278
7	Posterior basal LV	0.033	0.026	0.217	−0.374	0.035	−0.926
8	Lateral LV	0.045	0.055	0.222	−0.707	0.707	0.0
9	Anterior basal RV	0.097	−0.005	0.248	0.888	−0.400	0.222
10	Posterior basal RV	0.074	−0.020	0.206	−0.025	−0.492	−0.869
11	Anterior RV	0.095	0.015	0.212	0.949	−0.316	0.0

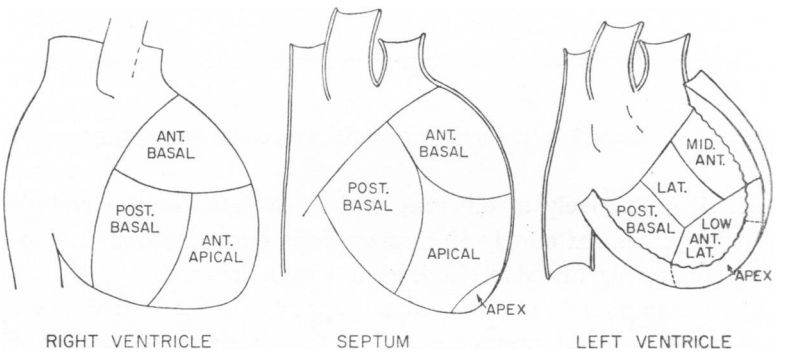

FIGURE 1 Myocardial segments represented by the 11 dipole set.

affect the dipole strengths. We shall demonstrate that the results are relatively insensitive to lead placement errors and recording artifacts (see Reliability of Results for One Subject) on account of the degree of over-determination of the process. For normal subjects, and for patients with certain hypertrophies, we usually obtain dipole strength curves with single peaks (see Dipole Strength Results). This is a result of our analysis and not an imposed constraint.

On each subject, potentials at 126 surface locations were recorded. This large number of recordings is not essential to our technique (see Reliability of Results for One Subject). In practice it appears that three or four times as many recordings as dipoles will suffice. However, in these early experiments we wish to ensure that our results are not influenced by numerical ill-conditioning or recording artifacts, and hence we overdetermine the problem by a factor of around ten.

Various subsets of the 126 recordings were used as input data. Since only eight channels could be recorded simultaneously (because of equipment limitations), one lead was kept fixed and used as a time reference. The remaining seven leads

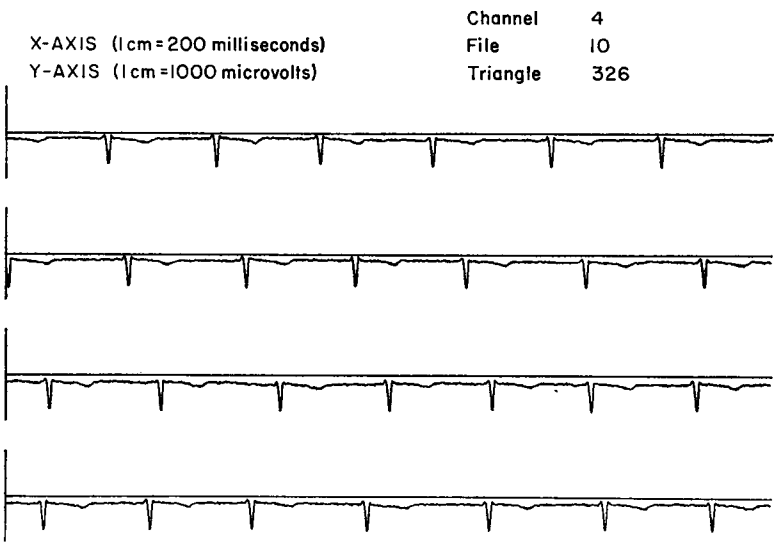

FIGURE 2 Example of raw surface potential data (amplifier polarity reversed).

were connected successively to different surface elements until a complete set of data was built up. Approximately 30 cardiac cycles were recorded at each location. The original analog signals were digitized at 1 msec intervals and stored on magnetic tape. An example of these "raw data" appears in Fig. 2. The raw data were then edited using a digital computer. Adjustments were made for the differences in amplifier gain between channels and for drift of the zero level of potential. This was done by taking zero potential for each lead and each cardiac cycle as an average of the recorded values between 310–290 msec prior to the timing indicator. The data for each cardiac cycle were then adjusted by a linear interpolation between successive zero points. Finally, approximately 20 cardiac cycles covering 3–5 respiratory cycles for each surface element were averaged together (the reference lead acting as a timing indicator) to give potentials at millisecond intervals

for the particular surface element. These were the "refined data" for one cardiac cycle for that surface element. Fig. 3 shows refined data corresponding to the raw data in the Fig. 2.

The location of the reference lead on a given subject was chosen such that the wave form had a distinct, sharp peak, either positive or negative as convenient; for any particular individual this peak may have been either a Q wave or an R wave, thus leading to differences or timing of up to 20 msec from subject to subject. This

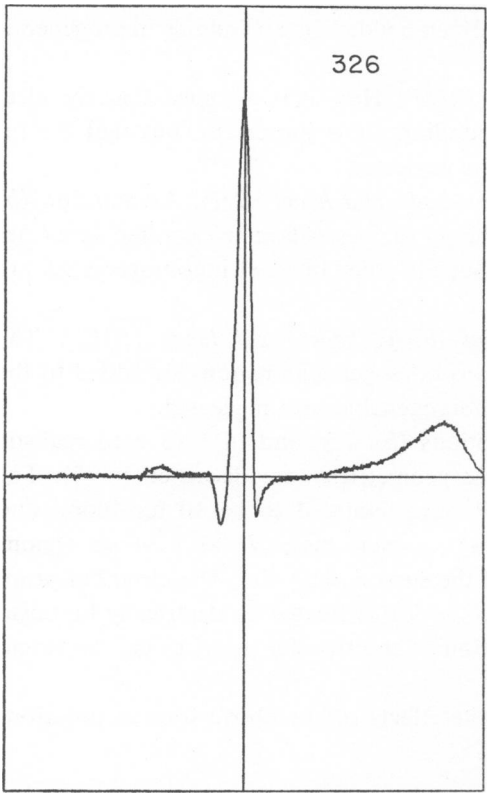

FIGURE 3 Refined surface potential data obtained from the raw data in Fig. 2. Only 600 msec of the cardiac cycle is shown so that the potential does not return to zero at the righthand side of the graph.

is noticeable when, for example, one compares the results of the repeat recordings made on the same individual (see Reliability of Results for One Subject). Thus only the relative timings are significant, the zero of time being arbitrary.

MODELS FOR THE TORSO

The transfer matrix **T** depends on the electrical model assumed for the torso, but the same transfer matrix can be used for all subjects with similar anatomy. Thus only a few such matrices would have to be precomputed. In our experiments, we have confined attention to subjects of the same age group and similar geometries,

and thus we have used transfer matrices corresponding to identical geometry for all subjects.

One of the objectives of this paper is to study the effect upon the inverse problem of different assumptions concerning electrical inhomogeneities. Thus, for the standard geometry, we have used four different transfer matrices, one for each of the following electrical assumptions:

(*a*) *Infinite homogeneous medium* (*IHM*). The effect of differing electrical properties between, for example, the body and the surrounding air is neglected and it is assumed that the source is effectively embedded in an infinite homogeneous medium.

(*b*) *Finite homogeneous medium* (*FHM*). Here it is assumed that the electrical difference between body and surrounding air is important, but that the internal inhomogeneities in the body may be neglected.

(*c*) *Finite inhomogeneous medium—body and heart* (*BH*). Assumption (*b*) is modified to include the effect of the blood masses within the cardiac ventricles (treated as two homogeneous regions), but all other internal inhomogeneities are neglected.

(*d*) *Finite inhomogeneous medium—body, heart, and lungs* (*BHL*). The electrical effect of the lungs (treated as two homogeneous regions) is added to the effects included in (*c*), but all further inhomogeneities are neglected.

When implementing modeling assumptions (*b*), (*c*), and (*d*), we used realistic geometry for the regions involved. These geometries were discussed in (2). The conductivities, relative to "body tissue," were assumed to be 10 for blood and $\frac{5}{8}$ for lung (19, 23, 24). Thus, in the most complete case, (*d*), we have six regions (two lungs, two ventricles, the body, and the surrounding air). The electrical properties vary from region to region, but each region is treated as electrically homogeneous. A full discussion of the computation of the transfer matrices can be found in (2, 15, 16).

In the next section we shall consider the effects of the above four assumptions upon the solution of the inverse problem.

DIPOLE STRENGTH RESULTS—EFFECT OF THE TORSO MODELING ASSUMPTIONS

An exhaustive study of the effects of all possible parameter variations on all results is beyond the scope of this paper. The results presented in this section were obtained from a single set of measurements on subject CM and are representative of our experience. The time-varying strengths of the 11 dipole set were obtained from the data, using the transfer matrices for the modeling assumptions described under Models for the Torso.

For comparison purposes we first present the results of an unconstrained fit, i.e., a fit in which the dipoles are permitted to have positive or negative strengths.

The dipole strengths as a function of time are shown in Fig. 4, but they bear little relation to the known features of the depolarization process (20, 21). We have consistently found this to be the case when using unconstrained fitting with in vivo (as opposed to simulated) data. All other results in this paper have the dipole strengths constrained nonnegative.

In Fig. 5, the constrained dipole strengths are plotted against time. The dotted curves were obtained with the IHM assumption, the dashed curves with FHM,

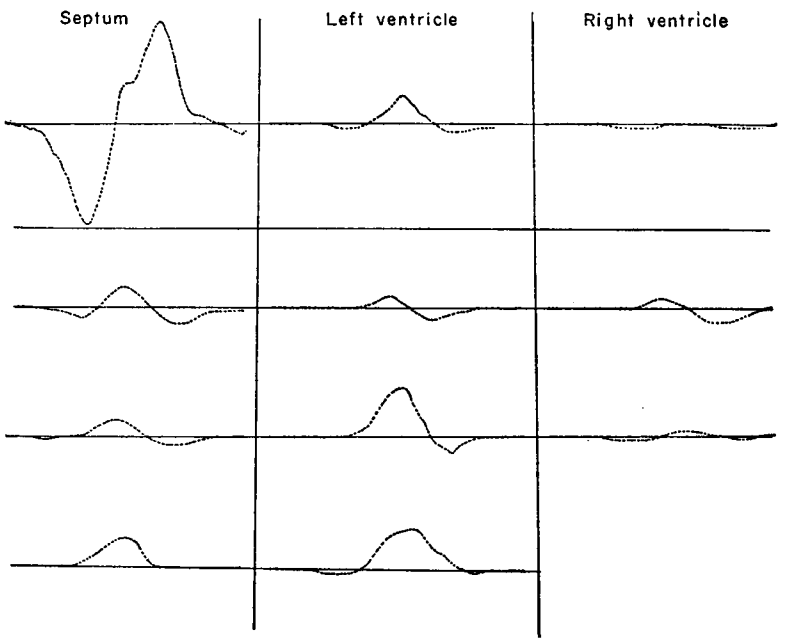

FIGURE 4 Unconstrained dipole strengths as a function of time for subject CM. The leftmost column contains the four septal dipoles (1, 2, 3, and 4—see Table I), the center column the four left ventricular dipoles (5, 6, 7, and 8), and the rightmost column the three right ventricular dipoles (9, 10, and 11). The strength scale is the same for all dipoles. The time scale spans 100 msec, including the QRS interval.

the dot-dash curves with BH, and the solid curves with the BHL assumption. The septal and the apical dipoles are shown in Figure 5 *a*, the left ventricle dipoles in Figure 5 *b*, and the right ventricular dipoles in Figure 5 *c*. Note that the amplitudes of the right ventricular dipoles are lower than those in other regions of the heart. The dipole strengths mostly have the form of a single pulse in time. This is the way we expected the model to reflect the physiology of myocardial excitation. The single pulses were obtained even though no time constraints were imposed, i.e., the curves were not constrained to have any particular functional form (in contrast to the work in reference 4). Exceptions to the single-pulse form are seen in dipoles 9 and 11, which seem to have two phases of activity. It is reasonable to suppose that the

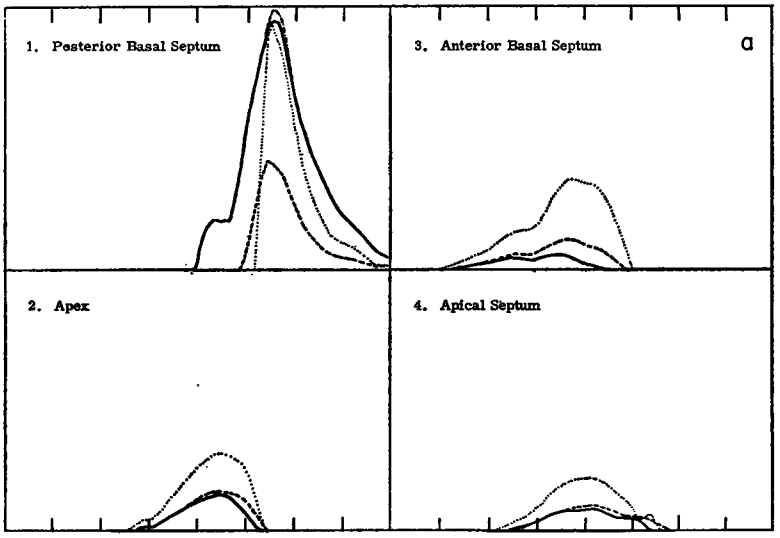

FIGURE 5 *a* Effect of torso modeling assumptions on the dipole strengths (constrained nonnegative) as a function of the time for subject CM. The four septal dipoles are shown. The dotted curves are for IHM, the dashed curves FHM, the dot-dash curves for BH, and the solid curve for BHL torso models. The strength scale is the same for all dipoles, full scale being 64 $\times$ 10^{-15} coul m (the dielectric constant of myocardium was taken as 80). The time scale spans 100 msec, including the QRS interval.

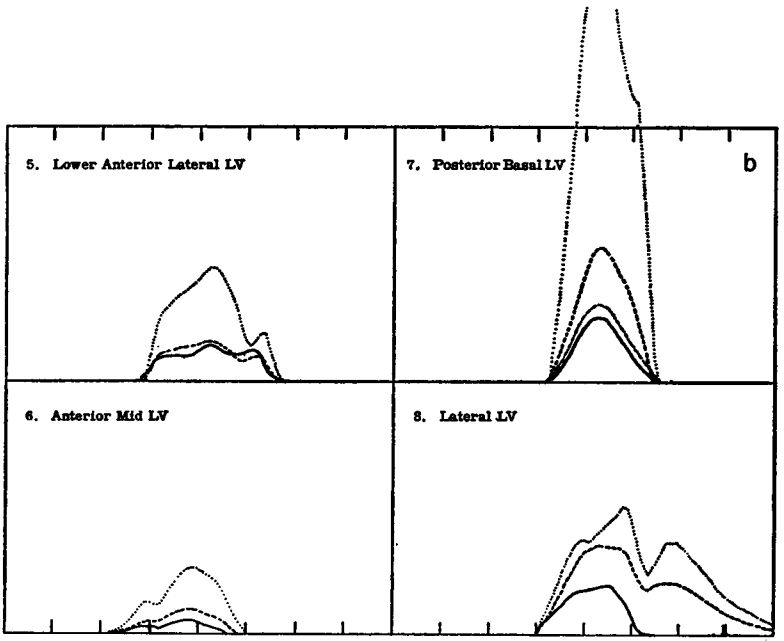

FIGURE 5 *b* Effect of torso modeling assumptions on the dipole strengths (constrained nonnegative) for the four left ventricular locations. Rest of caption same as for Fig. 5 *a*.

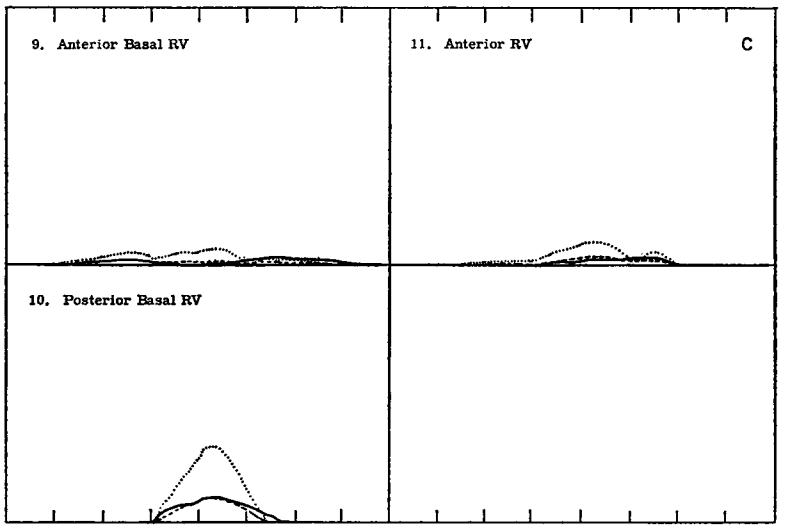

FIGURE 5 *c* Effect of torso modeling assumptions on the dipole strengths (constrained nonnegative) for the three right ventricular locations. Rest of caption same as for Fig. 5 *a*.

earlier phase represents right-directed septal activity and the later phase is the true right ventricular activity. (This will be discussed in greater detail under Discussion of the Activation Sequence).

It appears from Fig. 5 that the more realistically the torso is modeled, the more reasonable the dipole strengths appear. For instance, the activity of the lateral LV dipole (No. 8) persists for over 60 msec if assumption (*a*) or (*b*) is used, but cuts off as expected using assumptions (*c*) or (*d*). There is, in fact, little choice between (*c*) and (*d*); we choose to work with (*d*) (i.e. BHL) for the remainder of the paper since BHL is closest to anatomical reality. However, this may not be essential to future clinical implementation of this method.

It is instructive to take the time-integral of the dipole strength, since it might reasonably be assumed (see Variation of Time-Integrated Dipole Strengths between Individuals) that this quantity should be proportional to the volume of viable myocardium represented by each dipole. The results for subject CM, using the BHL assumption, are shown in Table II. The integrals for the right ventricular dipoles are much smaller than those for dipoles in other regions of the heart, which is consistent with the distribution of muscle.

As discussed under The Method, the dipole strengths shown in Fig. 5 are those which give a best fit to the surface potential data. It is important to investigate how good this "best fit" is, by recomputing surface potentials from the dipole strengths obtained. The recomputed potentials v^c for a few surface locations are compared with the measured potentials v in Fig. 6 (subject CM, BHL assumption), and it can be seen that the fit is reasonable. The locations chosen for this figure are described in the figure caption.

Taking into account all 126 surface locations, the RMS deviation between v^c and v in this case is 31 %. It might be noted that the corresponding RMS deviation for an unconstrained fit (which should, of course, be lower) is 21 %.

TABLE II

TIME-INTEGRATED DIPOLE STRENGTHS FOR THREE REPETITIONS ON SUBJECT CM

Units of 10^{-15} coul m sec or 5×10^{-8} amp m sec BHL torso modeling assumption

Dipole	Repetition		
	1	2	3
Septum			
1	1.01	1.10	1.08
2	0.12	0.06	0.04
3	0.08	0.10	0.09
4	0.10	0.23	0.18
Total	1.32	1.50	1.38
LV			
5	0.17	0.24	0.23
6	0.06	0.05	0.07
7	0.19	0.17	0.21
8	0.19	0.19	0.10
Total	0.61	0.64	0.61
RV			
9	0.06	0.09	0.06
10	0.11	0.13	0.11
11	0.05	0.03	0.03
Total	0.22	0.25	0.20
Total	2.15	2.39	2.20

RELIABILITY OF RESULTS FOR ONE SUBJECT

In this section, we discuss matters related to the reliability of the dipole strengths deduced from surface potential data.

A matter of practical importance is that of the reproducibility of results. This has been studied by repeating the recordings on subject CM, so that three sets of measurements were made on this subject at approximately one week intervals. The dipole strengths derived from the three sets of data (using the BHL assumptions) are shown in Fig. 7. It can be seen that the amplitudes of the dipoles reproduce well. Fig. 7 also shows that the relative timing of the dipoles is very consistent between

repetitions. The relative times of initial activity and of peak amplitude of the dipoles reproduce to within a few milliseconds. We can also compare the values of the time integrals of dipole strength for the three repetitions. These numbers are shown in Table II and the good agreement is again evident.

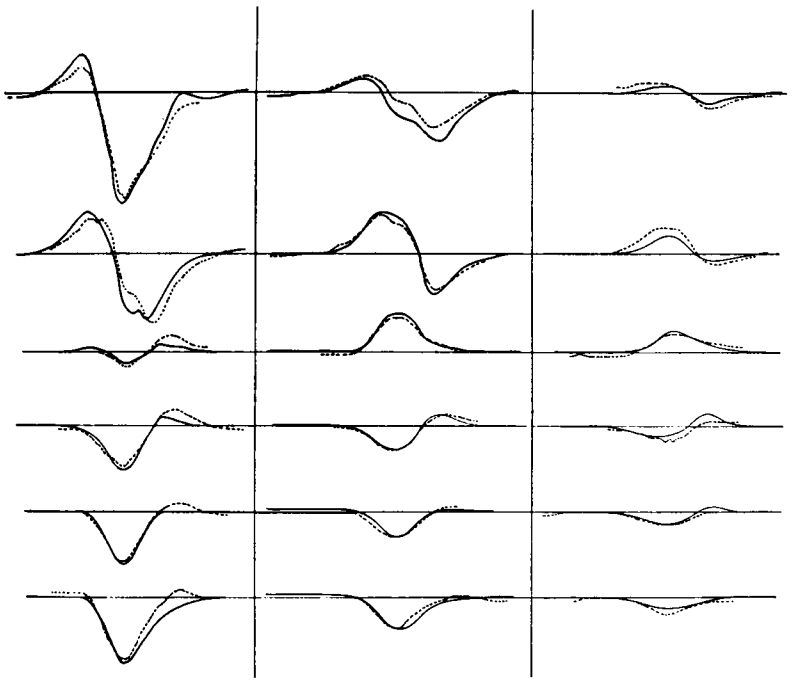

FIGURE 6 The surface potentials measured experimentally on subject CM are shown as a function of time by the dashed curves. The solid curves are surface potentials recomputed from the constrained nonnegative dipole strengths corresponding to the BHL torso modeling assumption as shown in Fig. 5. The surface locations chosen from three horizontal bands, which are arranged as columns on the figure. The leftmost column is the band at the level of the second intercostal space, the center column is at the sixth intercostal level, and the rightmost column at the first lumbar level. Within each column the order is (from top to bottom of column) center chest, left chest, left side, right back, right side, and right chest.

Another practical question is the number of surface points at which potentials must be measured. An obvious lower limit for the solution to be unique is $I = K$, but this would only yield meaningful results if perfect, noise-free data were available and the model were perfect. In reality, some degree of overdetermination is necessary. The results in the previous paragraph were obtained with $I = 126$, $K = 11$, an overdetermination factor of more than 10. In Fig. 8, the results are shown using subsets of the data, i.e. for $I = 60$, $I = 30$ and $I = 15$, obtained by deleting approximately every second surface location from the next larger set.

The $I = 60$ subset produces dipole strengths little different from those obtained from the full set. However, the smallest subset, $I = 15$, gives rather ragged curves. Apparently an overdetermination factor of about four is satisfactory.

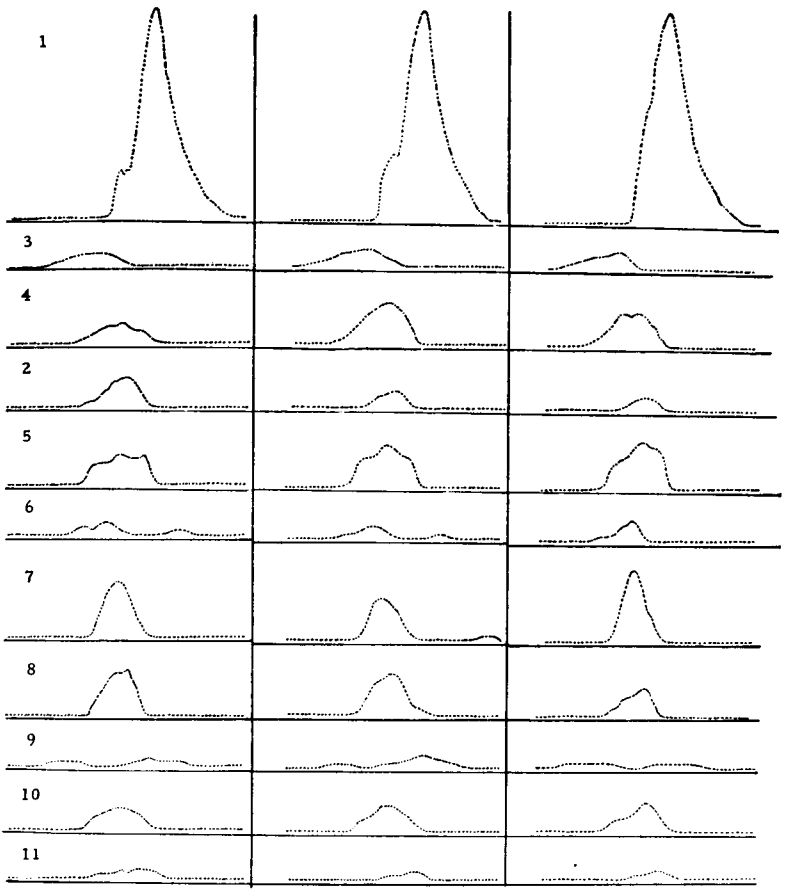

FIGURE 7 Dipole strengths (constrained nonnegative) obtained from repeated surface potential measurements on subject CM. The interval between the repetitions was approximately one week. Results from the three sets of data are arranged in columns. The strength scale is nearly the same for the three columns, full scale being 3.8, 3.9, and 3.2 for columns 1–3 respectively in units of 10^{-6} amp m. Within a column the scale is constant. From top to bottom the dipole sequence is 1, 3, 4, 2, 5, 6, 7, 8, 9, 10, 11. The time scale covers 100 msec, including the QRS interval.

To simulate the effect of lead misplacement, a series of computations were made in which incorrect surface locations were input to the program. Since the surfaces are triangularized (2), this was easily done by misstating the identifying number of the triangle at which a particular set of potential data were measured. Three misplacement schemes were used: (*a*) for 90% of the triangles, identifying numbers of

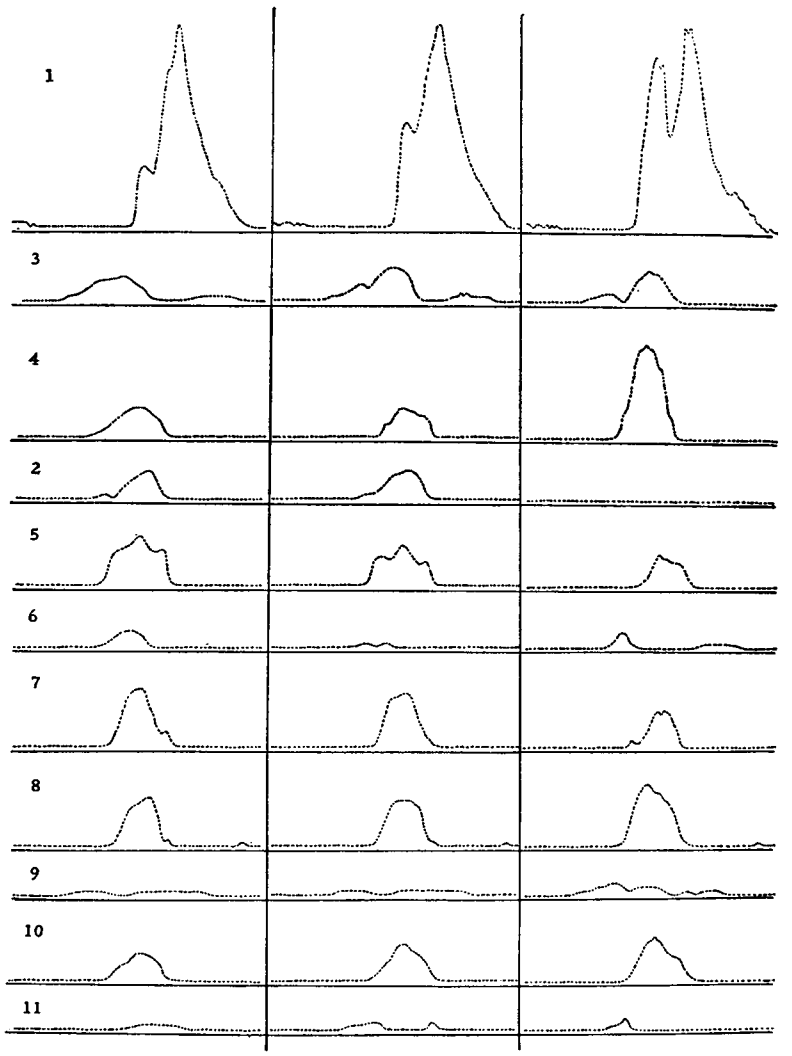

FIGURE 8 Dipole strengths (constrained nonnegative) obtained from subsets of the first set of surface potential measurements on subject CM. The leftmost column was obtained using potentials 60 surface locations, the center column 30 locations, and the rightmost column 15 locations.

immediately adjacent triangles were substituted, the direction of the change being random. (*b*) for all triangles identifying numbers of triangles up to 3 inches away were substituted. (*c*) for all triangles identifying numbers of triangles up to 5 inches away were substituted.

The results for the time-integrated dipole strengths for subject CM are presented in Table III. The strengths are affected by these fairly severe lead misplacements,

TABLE III

TIME-INTEGRATED DIPOLE STRENGTHS RESULTING FROM LEAD MISPLACEMENT ON SUBJECT CM

Units of 10^{-15} coul m sec or 5×10^{-8} amp m sec BHL torso modeling assumption

		Misplacement scheme		
Dipole	Original	(a)	(b)	(c)
Septum				
1	1.01	0.74	0.75	0.74
2	0.12	0.08	0.04	0.02
3	0.08	0.08	0.16	0.20
4	0.10	0.13	0.00	0.09
Total	1.32	1.03	0.95	1.04
LV				
5	0.17	0.20	0.28	0.20
6	0.06	0.10	0.02	0.03
7	0.19	0.21	0.20	0.27
8	0.19	0.15	0.19	0.18
Total	0.61	0.66	0.68	0.67
RV				
9	0.06	0.02	0.03	0.09
10	0.11	0.10	0.08	0.09
11	0.05	0.02	0.08	0.02
Total	0.22	0.15	0.20	0.20
Total	2.15	1.83	1.82	1.91

but the change is not drastic compared to the variations to be discussed under Variation of Time-Integrated Dipole Strengths between Individuals.

The differences between the three repeated measurements on subject CM are somewhat less than the changes seen in the lead misplacement studies. This implies that our techniques for placing the leads at definite triangles are quite accurate.

DISCUSSION OF THE ACTIVATION SEQUENCE

In this section we compare our results with the expected sequence of activation in normal subjects.

The excitation of the myocardium has been investigated by a number of research groups using penetrating electrodes. Such measurements have been made on dogs, monkeys, and, to a lesser extent, on humans. They have been reviewed by Scher (20, 21), who finds general agreement between the results of the various groups, although there are some differences.

For reference we review the general sequence of activation in primates. The earliest activity starts at the mid-left septal surface, producing a wave in the septum directed to the right, towards the head and slightly anteriorly. It is followed shortly by the second phase, which is inside-out activity of the middle- and apical-left free wall. The third phase, beginning later in time in the primates than in the lower animals, includes outward activity in the right wall and further outward activity in the left wall. The activity of the basal portion of the heart begins later and the latest activity is in the basal septum.

TABLE IV

COMPARISON OF EXPERIMENTALLY DETERMINED ACTIVATION SEQUENCE (SCHER) AND COMPUTED DIPOLE ACTIVITY

Activation sequence according to Scher			Computed sequence of dipole activity (BHL torso modeling assumption, subject CM)	
Phase	Description	Dipoles	Dipole	Relative time
				msec
I	Wave in septum, rightward superiorly and anteriorly	3, 4, 9*a*, 11*a*	9*a*	0
			3	2.5
II	Inside to outside mid- and apical-left free wall	2, 5, 6, 8	11*a*	4
III	Inside to outside right free wall	9*b*, 10, 11*b*	4	13
			6	18
IV	Posterior left wall and basal septum	1, 7	2, 5	24
			8, 10	25
			7	26
			11*b*	30
			1	32
			9*b*	34

In dogs, the depolarization sequence is complicated by the observation of appreciable "reversals," that is, right-to-left activity in the septum and inward activity in the subendocardium. However, these effects were found to be substantially smaller in the monkey. This should improve the appropriateness of our constrained dipole set, which would not include reversal effects.

On the basis of the activation sequence given above, the sequence of onset of activity of the dipole set would be expected to be that shown in Table IV. In our experiments, for the three repetitions on subject CM (Reliability of Results for One Subject) a very consistent sequence of activation was determined. Both the onset

and peak times were reproduced to within a few milliseconds. The times of onset of activity for the computed dipoles are also shown in Table IV. The right ventricular dipoles 9 and 11 show two phases of activity. These have been denoted as *a* and *b* in Table II, and it seems reasonable to associate the earlier phase with right-pointing septal activity and the later phase with the right ventricular activity. Possibly an

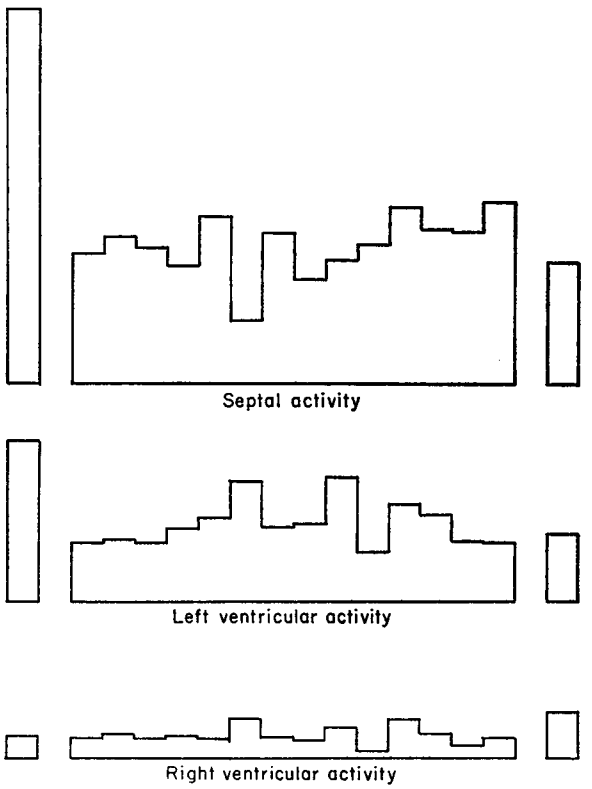

FIGURE 9 Bar chart of integrals under the dipole strength versus time curves. The sums of the integrals for the four septal dipoles are at the top level, for the four left ventricular dipoles on the next level, and the three right ventricular dipoles on the lowest level. The center block is for the twelve normal subjects, the three repetitions of subject CM being shown at the left extreme of this block. Normal ranges for the quantities are indicated by this chart. On the far left, values are shown for a patient with left ventricular hypertrophy. On the far right values are shown for a patient with right ventricular hypertrophy.

improved dipole set would remove this effect. We have experimented briefly in this direction, adding a right-pointing dipole in the anterior low septum; the early activity of dipoles 9 and 11 appeared on this additional dipole, but so did some of the later activity.

This suggests that our separation of activity should be regarded more as a separation of the source into its directional components than as a spatial separation.

This is consistent with the firing of dipole 3, which is slightly earlier than would be expected of a dipole at this location although approximately as expected of a dipole with this direction. Thus, we are led to consider the implications of being able to separate the source into its directional components, without being completely able to separate it spatially.

With normal depolarization sequence, we have seen that to a considerable degree we can associate the directional separation of the source with anatomical location, since depolarization generally proceeds from endo- to epicardium. There is some

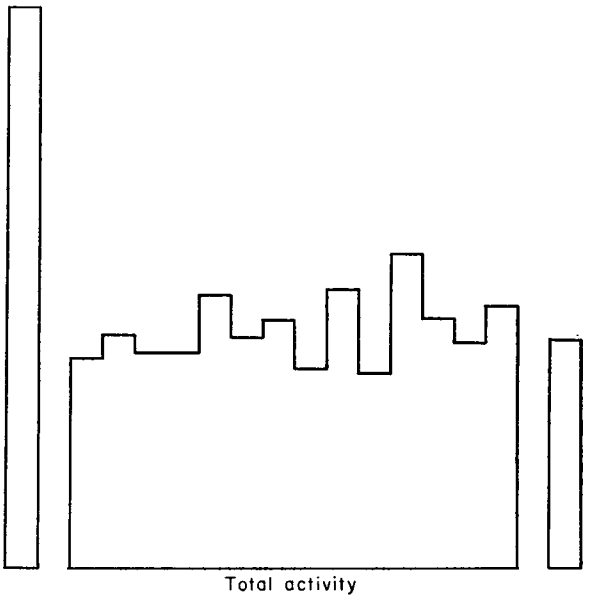

FIGURE 10 Bar chart of the sum of the time integrals for all eleven dipoles. The center block is for the twelve normal subjects, the value for the LVH patient is on the left, and that for the RVH patient is on the right.

confusion between the septum and the right ventricle, although we can separate the early and later activity in dipoles 9 and 11.

This approach may not be satisfactory for patients with abnormal depolarization sequences. We expect that these would give clearly abnormal dipole strengths which could not be associated with localized anatomical activity. An unconstrained fit might then be studied.

VARIATION OF TIME-INTEGRATED DIPOLE STRENGTHS BETWEEN INDIVIDUALS

We now briefly discuss partial results for twelve normal subjects and two patients, one with left ventricular hypertrophy (LVH) and one with right ventricular hyper-

trophy (RVH). The patient with LVH had severe aortic stenosis. Although the RVH patient had moderately severe mitral stenosis and clinical, X-ray and surgical evidence of RVH, the electrocardiographic and vectorcardiographic QRS was within normal limits. The normal subjects were chosen to be similar in size and age and so were assumed (for computational purposes) to be geometrically identical. Thus the same **T** matrices were used for all.

The time-integrated dipole strengths (BHL assumption) were obtained for each individual. The sum of the integrals for the four septal dipoles should (25) be a measure of the volume of viable myocardium in the septum. The sums of the four LV dipoles and of the three RV dipoles have a corresponding interpretation. Finally, the sum of all eleven integrals should be a measure of the total myocardial volume.

The results for the summed integrals are presented in Figs. 9 and 10. It can be seen that there is variation among the twelve normal subjects. This is as expected, because of the usual variation within a biological sample and particularly since the boundaries of each myocardial segments are not precisely defined. However, a "normal range" exists for the four quantities defined above. In contrast, the LVH patient has abnormally high septal, LV, and total sums but normal RV. On the other hand, the RVH patient is high in the RV.

CONCLUSIONS

The objective of this study is to solve the restricted "inverse problem" and determine the time-varying strengths of a dipole set from surface potential data. It is difficult to prove that this has been accomplished, since there exists no simple independent methods for determining the dipole strengths. However, there are three pieces of evidence that suggest that the model and the dipole strengths we obtain are meaningful and that this approach merits further consideration. Firstly, we obtain for normal human subjects a similar depolarization sequence to that found using penetrating electrodes. Secondly, our results for patients independently diagnosed as having left and right ventricular hypertrophy are consistent with what is expected for these abnormalities. Thirdly, the overdetermination factor ensures that the results are not significantly affected by errors in lead placement or recording artifacts. This third point would presumably be operative, to a greater or lesser extent, with other possible models.

SUMMARY

After studying the "forward problem" of electrocardiology in previous papers, we turned to the study of the "inverse problem." Using in vivo surface potential measurements, we obtained the time-varying strengths of 11 dipoles representing the heart electrically. The results appeared physiologically reasonable and they encourage the hope that this approach may develop into a useful tool for studying ventricular infarction and hypertrophy.

The authors are especially grateful to Dr. Lloyd Hefner for his support, advice, and encouragement throughout all phases of this project. We are also extremely indebted to Messrs. P. Svendsen, M. B. McGrath, R. H. Crane, and K. Brush for producing the programs and running many of the calculations on which this paper is based, and would also like to thank A. Spear and G. Stefanu, and Drs. L. Axsom and W. H. Lyne, IV, for their assistance on recording and A/D techniques. The continuing helpful advice of Dr. J. W. Evans has been particularly appreciated.

The work at the University of Alabama Medical Center was supported by NIH Grants HE-10885 and HE-09423, and by a grant from the Alabama Heart Association.

Received for publication 5 June 1967.

REFERENCES

1. BARNARD, A. C. L., I. M. DUCK, and M. S. LYNN. *Biophys. J.* **7**:443.
2. BARNARD, A. C. L., I. M. DUCK, M. S. LYNN, and W. P. TIMLAKE. *Biophys. J.* **7**:463.
3. BARR, R. C., T. C. PILKINGTON, J. P. BOINEAU, and M. S. SPACH. 1966. *I. E. E. E. (Inst. Elec. Electron. Engrs.), Trans. Bio-Med. Eng.* **13**:88.
4. BELLMAN, R., C. COLLIER, H. KAGIWADA, R. KALABA, and R. SELVESTER. 1964. *Comm. ACM.* **7**:666.
5. BOINEAU, J. P., M. S. SPACH, T. C. PILKINGTON, and R. C. BARR. 1966. *Circulation Res.* **19**:489.
6. BRODY, D. A., J. C. BRADSHAW, and J. W. EVANS. 1961. *I.R.E. (Inst. Radio Engrs.), Trans. Bio-Med. Electron.* **8**:139.
7. GELERNTER, H. L., and J. SWIHART. 1964. *Biophys. J.* **4**:285.
8. GELERNTER, H. L., and J. SWIHART. 1965. Electrophysiology of the Heart. B. Taccardi and G. Marchetti, editors. Pergamon Press, Inc., New York.
9. GELERNTER, H. L., and J. SWIHART. 1965. Proceedings of the 3rd All-Union Conference on Automatic Conference on Automatic Control and Technical Cybernetics, Odessa, U.S.S.R., 1965.
10. GESELOWITZ, D. B. 1961. *Proc. I.R.E. (Inst. Radio Engrs.),* **48**:75.
11. HORAN, L. G., and N. C. FLOWERS. 1967. *Med. Res. Eng.* **6**:28.
12. HORAN, L. G., N. C. FLOWERS, and D. A. BRODY. 1963. *Circulation Res.* **13**:373.
13. KIRK, W. L., JR., R. H. SELVESTER, and C. COLLIER. 1966. Engineering in Medicine and Biology. Proceedings of the 19th Annual Conference, San Francisco, Calif. 192.
14. LYNN, M. S., J. H. HOLT, JR., W. H. LYNE, J. W. EVANS, L. L. HEFNER, and L. T. SHEFFIELD. 1967. 25th Annual Meeting, Southern Society for Clinical Research, New Orleans, 1967. *Clin. Res.* **15**:56.
15. LYNN, M. S., and W. P. TIMLAKE. Numerische Mathematik. To appear.
16. LYNN, M. S., and W. P. TIMLAKE. *J. Soc. Ind. Appl. Math. Ser. B.* (Numerical Analysis). To appear.
17. PLONSEY, R. 1966. *Bull. Math. Biophys.* **28**:161.
18. POZZI, L. 1961. Basic Principles in Vector Electrocardiography. Charles C. Thomas, Publisher, Springfield, Ill.
19. RUSH, S., J. A. ABILDSKOV, and R. MCFEE. 1963. *Circulation Res.* **12**:40.
20. SCHER, A. M. 1962. *In* Handbook of Physiology. W. F. Hamilton and P. Dow, editors. American Physiological Society, Washington, D.C. **1**:287.
21. SCHER, A. M. 1965. *In* Electrophysiology of the Heart. B. Taccardi and G. Marchetti, editors. Pergamon Press Ltd., London. 217.
22. SCHULER, G. 1966. Symposium on Biomedical Engineering, Milwaukee, Wisc., 1966.
23. SCHWANN, H. P., and C. F. KAY. 1956. *Circulation Res.* **4**:664.
24. SCHWANN, H. P., and C. F. KAY. 1957. *Circulation Res.* **5**:439.
25. SELVESTER, R. H., C. R. COLLIER, and R. B. PEARSON. 1965. *Circulation.* **31**:45.
26. SELVESTER, R. H., J. C. SOLOMON, and T. L. GILLESPIE. 1966. Presented at 39th Scientific Seminar of the American Heart Association, 1966. *Circulation Suppl. 3.* **33**:212.
27. TACCARDI, B. 1966. *Circulation Res.* **19**:865.
28. WOLFE, P. 1959. *Econometrica* **27**:382.